MDPI

Review

Bioorthogonal "Click" Cycloadditions: A Toolkit for Modulating Polymers and Nanostructures in Living Systems

Irene Lepori [1], Yavuz Oz [2], Jungkyun Im [3,4], Nandan Ghosh [3], Mohuya Paul [3], Ulrich S. Schubert [5,6] and Stefano Fedeli [5,6,*]

[1] Department of Microbiology, University of Massachusetts Amherst, 639 North Pleasant Street, Amherst, MA 01003, USA
[2] Department of Chemical and Biomolecular Engineering, University of California Los Angeles, Los Angeles, CA 90095, USA
[3] Department of Electronic Materials, Devices, and Equipment Engineering, Soonchunhyang University, Asan 31538, Republic of Korea
[4] Department of Chemical Engineering, Soonchunhyang University, Asan 31538, Republic of Korea
[5] Laboratory of Organic and Macromolecular Chemistry (IOMC), Friedrich Schiller University Jena, Humboldtstr. 10, 07743 Jena, Germany
[6] Jena Center for Soft Matter (JCSM), Friedrich Schiller University Jena, Philosophenweg 7, 07743 Jena, Germany
* Correspondence: stefano.fedeli@uni-jena.de

Abstract: "Click" cycloadditions offer effective pathways for the modifications of supramolecular structures, polymers, and nanomaterials. These reactions include bioorthogonal mechanisms that do not interfere with the biological processes, providing a type of chemistry to operate directly in living environments, such as cells and animals. As a result, the "click" cycloadditions represent highly and selective tools for tailoring the properties of nanomedicine scaffolds, expanding the efficacy of multiple therapeutic strategies. We focused this minireview on the bioorthogonal cycloadditions, presenting an insight into the strategies to modify nanostructured biomedical scaffolds inside living systems. We organized the contributions according to the three main mechanisms of "click" cycloadditions: strain-promoted sydnone-alkyne, tetrazine ligation, and strain-promoted [3+2] azido-alkyne.

Keywords: cycloaddition reactions; polymers; nanomaterials; bioorthogonal chemistry; click chemistry

1. Introduction

Polymers and nanostructures offer platforms that can operate safely in living systems [1–3], enabling the development of localized treatments with enhanced efficacy [4–6]. The advantage of these structures is the biocompatible scaffold combined with the possibility to host different types of therapeutic payloads [7–9]. The surface functionalization of the materials can also provide fine-tuning of key properties such as water solubility [10,11], stealth behavior [12–14], fluorescence [15–17], and targeting ability [18–20]. These features are essential for applications in stimuli-responsive treatments [21–23], theragnostic [24–26], and in situ drug generation [27–30]. Different covalent and non-covalent approaches have been adopted for engineering nanomaterials [31–34]. Bioorthogonal chemistry offers reactions that do not interfere with native biological mechanisms, enabling dedicated pathways for modifying these platforms [35]. As a result, bioorthogonal transformations represent a unique toolkit for manipulating nanomaterials, polymers, and biomolecules directly inside living systems [36,37]. This approach opens access to highly specific and targeted ways for modulating the properties of the designed nanomedicine scaffold [38].

Multiple bioorthogonal reactions are based on "click" cycloadditions to overcome the challenges of achieving chemical modifications in the bioenvironment [39,40]. These

mechanisms can operate on nanostructures in aqueous solvents and under different conditions [41–43] without being affected by the presence of salts and proteins [44]. Applying these cycloadditions for modifying nanomaterials and polymers inside cells and living organisms facilitates improvements in the design and the accuracy of the resulting treatments.

In this minireview, we focused on the bioorthogonal "click" cycloadditions adopted to perform modifications inside living systems on biomedical scaffolds such as polymers and nanomaterials. Relevant applications on biomolecules were also included. We highlighted the features provided by the decorations and their role in achieving the biomedical goals. The contributions were organized according to the different reactions (Figure 1): strain-promoted sydnone-alkyne cycloaddition, tetrazine ligation, and strain-promoted [3+2] azido-alkyne cycloaddition. In consideration of this, we have narrowed the selection of seminal papers to reactions performed in actual biosystems. Nitrone-alkyne is a further type of cycloaddition that presents an early though important potential for bioorthogonal mechanisms, and significant cases of this reaction are briefly mentioned.
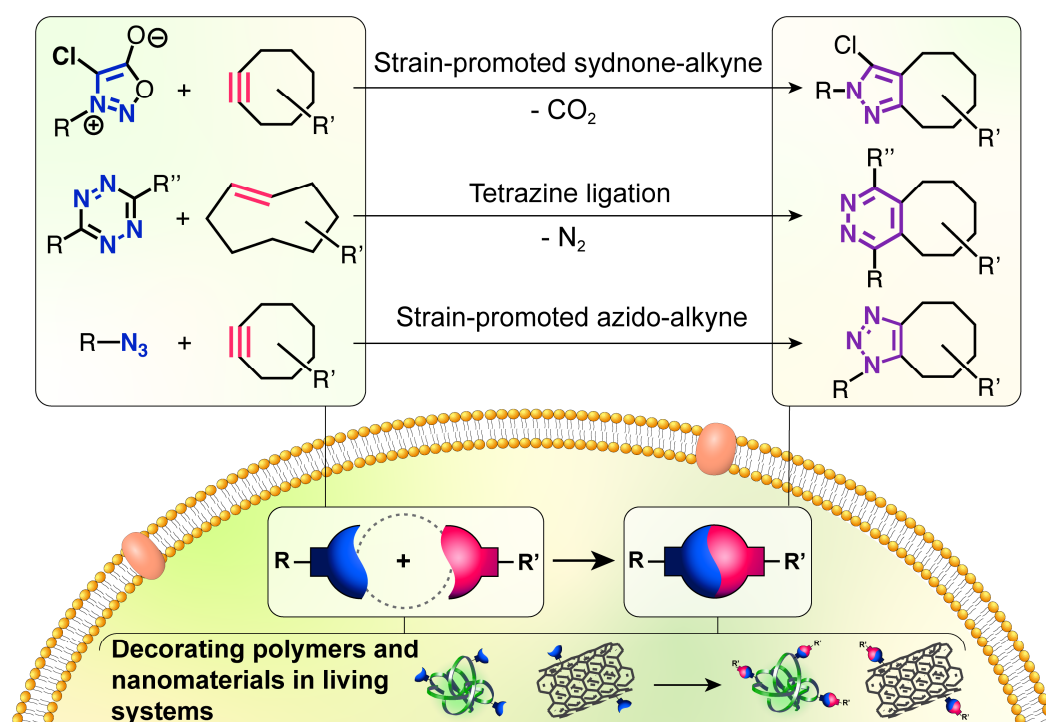

Figure 1. The three classes of bioorthogonal "click" cycloadditions studied for their ability to operate inside the living environment: strain-promoted sydnone-alkyne (SPSAC), tetrazine ligation, and strain-promoted azido-alkyne (SPAAC).

2. Strain Promoted Sydnone-Alkyne Cycloaddition—SPSAC

The potential of the strain-promoted sydnone-alkyne cycloaddition (SPSAC) was presented by Chin and coworkers in 2014 through the coupling between *N*-phenylsydnone and cyclooctyne. The pyrazole cycloadduct was obtained through a [3+2] cycloaddition followed by the elimination of CO_2 through a retro-Diels–Alder reaction [45]. The reaction efficiently worked in a buffer solution at physiological temperature without requiring metal catalysis. The use of this reaction, however, was limited by the small rate constant compared to other bioorthogonal reactions (e.g., SPSAC = 0.054 M^{-1} s^{-1} in MeOH/H_2O mixture, while SPAAC = 0.14 M^{-1} s^{-1}) [46]. Kolodych, Taran, and coworkers focused on overcoming this limitation by finding two key substitutions that increased the sydnone reactivity: A chlorine on C4 (chlorosydnone, Cl-Syd) and an electron-withdrawing group on the aryl bonded to the nitrogen (Figure 2) [47]. These key findings prompted its application within living systems.
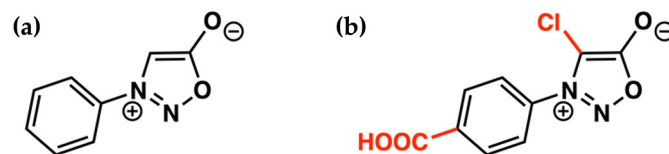
Figure 2. (**a**) Schematic representation of the originally proposed structure of the sydnone and (**b**) the higher reactive version.

Taran, Specklin, and coworkers introduced the in vivo use of the SPSAC reaction with Cl-Syd and cyclooctynes for imaging purposes through positron emission tomography (PET) [48]. First, the authors pretreated a xenograft model of a tumor-bearing nude mouse with sydnone-decorated Cetuzimab antibody (CTX-Syd, Figure 3) which targets the epidermal growth factor receptor, overexpressed in several cancer cells. After three days of CTX-Syd treatment, the fluorine-18 radiolabeled cyclooctyne ([18F]-2) was administered, enabling the SPSAC reaction in vivo. PET imaging revealed a significantly higher tumor accumulation of [18F]-2 in the sample pre-treated with CTX-Syd compared to the control treated with only [18F]-2, indicating the specificity and efficacy of the in vivo SPSAC coupling. This success opened several opportunities for adopting this cycloaddition in tumor-imaging techniques.

Figure 3. Schematic representation of the components developed by Taran, Specklin, and coworkers for the preparation of Cetuzimab-sydnone conjugate (CTX-Syd) and SPSAC reaction with [18F]-2 in physiological conditions to obtain radioactive [18F]-CTX-Pyr. (DCM = CH$_2$Cl$_2$). Adapted with permission from ref. [48]. Copyright 2019 Royal Society of Chemistry.

Gerke, Rubio-Retama, and coworkers, developed nanoparticles based on bovine serum albumin (BSA) and antibodies directed against the programmed death ligand 1 (PD-L1) [49]. PD-L1 is an important immune checkpoint inhibitor and exerts its function by binding its

specific receptor onto the immune cell surface. PD-L1 is overexpressed onto the surface of various cancer cell types, weakening the immune response upon binding to the receptor. Inhibiting the interaction between PD-L1 and its receptor through antibodies against PD-L1 is an effective strategy to restore a proper immune response against cancer tissues. The approach proposes a proof-of-concept study by generating BSA-based nanoparticles decorated with chlorosydnone (Cl-Syd) designed to react with the anti-PD-L1 antibody functionalized with the dibenzocyclooctyne (DBCO) group. The approach consists of first, in the interaction of the DBCO-functionalized anti-PD-L1 antibody with the cancer cell surface. Subsequently, the treatment with Cl-Syd-BSA nanoparticles leads to an in situ SPSAC reaction with the DBCO-antibody. The effectiveness of the cycloaddition in the pre-targeted approach was demonstrated in vitro against the non-small cell lung cancer human cell line H358 by using fluorescein isothiocyanate (FITC)-functionalized Cl-Syd-BSA nanoparticles. After treatment with the DBCO-anti-PD-L1 antibody, the incubation with FITC-Cl-Syd-BSA led to green fluorescence of the cell surface pre-treated with the DBCO-decorated antibody but not for the ones pretreated with the unmodified antibody, demonstrating the actual occurrence of SPSAC reaction on live cells in vitro.

Friscourt and coworkers demonstrated the applicability of the SPSAC reaction on proteins and glycans [50] and performed for the first time the cycloaddition on nucleosides and oligonucleotides within transfected cells [51]. Specifically, HeLa cells were transfected with sydnone-modified DNA and subsequently treated with the sulfo-Cyanine3 fluorescent dye conjugated to DBCO (sulfoCy3-DBCO). Confocal microscopy revealed a clear fluorescence in the cell cytoplasm, compared with the cells not transfected with the DNA. This research highlights the potential of the SPSAC reaction for labeling various biomolecules, including DNA, within cellular environments, offering a promising avenue for further studies and applications.

3. Strain Promoted [3+2] Azide-Alkyne Cycloaddition—SPAAC

The seminal application in the living system of the strain-promoted [3+2] azide-alkyne cycloaddition (SPAAC) was presented by Bertozzi and coworkers in 2004. This work showed the use of cyclooctynes for modifying biomolecules in living systems [52]. Despite its relatively slow kinetics compared to other bioorthogonal cycloadditions, the SPAAC reaction is one of the most employed bioorthogonal mechanisms in recent decades [53]. The azide group can be properly introduced into living systems by feeding a specific organism with azido-modified metabolic precursors [54]. The presence of the azide group as a chemical "handle" is a minor modification of biomolecules, easily tolerated by enzymes and metabolic mechanisms [55]. This biocompatibility, together with the fast-raising availability of azido- and strained alkyne derivatives, has widely promoted its employment for biomedical strategies impossible to approach with genetic methods. The SPAAC reaction has been extensively employed in combination with live therapeutics for cancer treatments. Several applications of this reaction show the modification of live immune cells, bacteria, and viruses, successfully enhancing the therapeutic potential of these organisms in preclinical trials [56].

Liu and coworkers developed nanoparticles formed by a zeolitic imidazolate framework-8 (ZIF-8) functionalized with dibenzyl cyclooctyne. These nanoparticles were attached with a cleavable linker (DSPE-PEG-SS-DBCO, Figure 4) to the surface of live *Escherichia coli*, pre-functionalized with azido group (Figure 3) [57]. Since various attenuated bacteria present a natural tropism for the immunocompromised and hypoxic tumor microenvironment, the attachment of nanoparticles on their surface can significantly improve the pharmacokinetics of nanoparticle-loaded drugs [58]. In preparing the assembly, the ZIF-8 nanoparticles were loaded with the chemotherapeutic drug doxorubicin and the photosensitizer indocyanine green. Subsequently, the nanoparticle's surface was decorated with dibenzyl cyclooctyne. This functionalization was performed via incubation with the linker DSPE-PEG-SS-DBCO, containing the cleavable disulfide group.
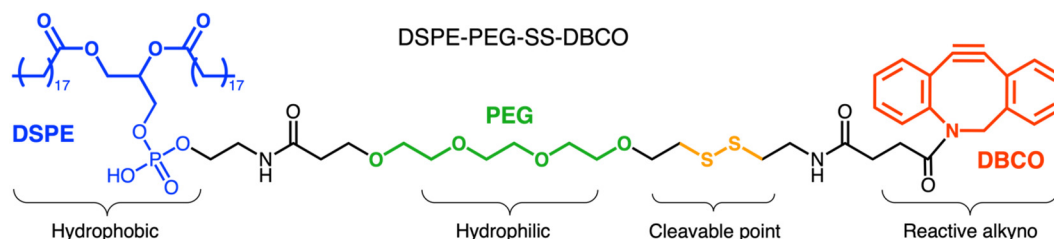
Figure 4. Schematic representation of the cleavable linker DSPE-PEG-SS-DBCO: Di-stearoyl-sn-glycero-3-phosphopthanolamine-poly(ethylene glycol)-SS-di-benzyl-cyclooctyne. This linker was adopted by Liu and coworkers [57].

The indocyanine green is used for photodynamic and photothermal therapy as this molecule yields a temperature increase and reactive oxygen species under near-IR laser radiation. The metabolic decoration of *E. coli* cell wall with the azide group was achieved by incubating the bacteria with azide-D-alanine. The bacteria intake of the D-alanine results in the incorporation of the azide-D-alanine on the last amino acid of peptidoglycan stem peptide within bacterial surface [59]. The generated microbial nanohybrid is subsequently connected to ZIF-8 pH-responsive degradable metal-organic framework nanoparticles. This bonding is based on a cleavable linker, sensitive to the tumor microenvironment. As a result, the therapeutic effect remains localized in the tumoral tissue. Overall, the efficacy of the bacteria–nanoparticles conjugate (*E. coli*@ZIF-8SS/I&D) was evaluated on a 4T1 murine breast carcinoma model (Figure 5). As controls are tested the individual components of the system. *E. coli*@ZIF-8SS/I&D revealed the strongest effect in reducing the tumoral volume. Importantly, *E. coli*@ZIF-8SS/I&D did not cause mice body weight loss or obvious damage in major tissues, indicating the safety of the approach.

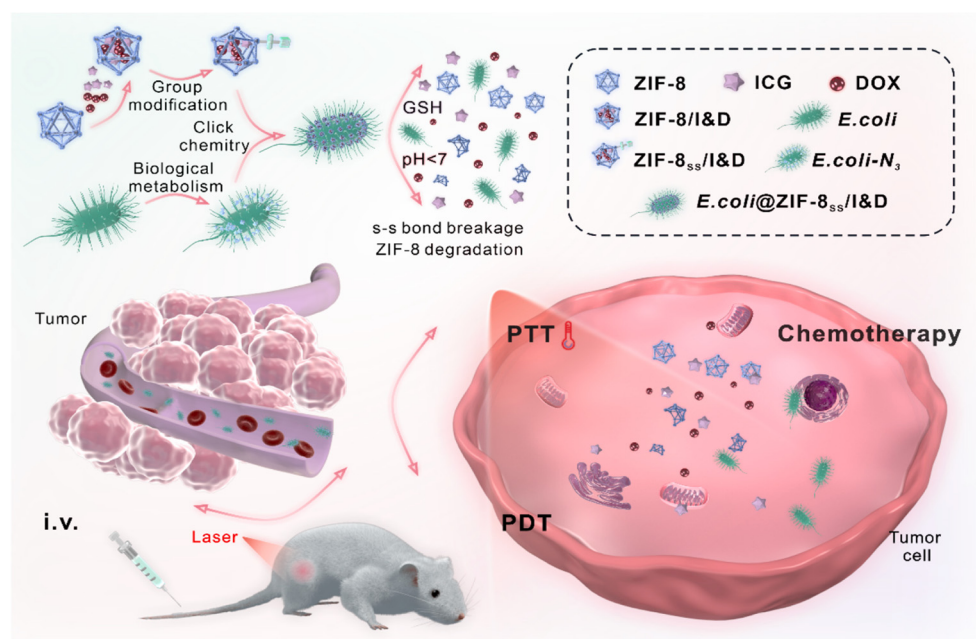

Figure 5. Schematic representation of the approach employed by Liu and coworkers with indocyanine green (ICG) and doxorubicin (DOX) embedded in ZIF-8 nanoparticle that, after functionalization with DSPE-PEG-SS-DBCO, are attached through SPAAC reaction to *E. coli* surface metabolically pre-functionalized with azido-group. This decoration generates *E. coli*-ZIF-8ss/I&D. The release of the

nanoparticles from bacterial surface is mediated by high concentrations of glutathione (GSH) in tumor cells cytoplasm, while the release of ICG and DOX drugs from ZIF-8 nanoparticles is mediated by their low intracellular pH. First, *E. coli*-ZIF-8ss/I&D selectively accumulate inside tumor tissue. After the release, the laser irradiation can exert the photodynamic (PDT) and photothermal therapy (PTT), while the doxorubicin provides the chemotherapeutic effect. Reprinted with permission from ref. [57]. Copyright 2022 Elsevier.

The in vivo performances of the SPAAC demonstrated the wide applicability of this bioorthogonal cycloaddition. Several strategies adopted azide and strained alkyne groups to mimic receptor–ligand interaction in vivo, improving the pharmacokinetic and significance of multiple live therapeutics [60]. The Cai group focused on functionalizing the surface of immune cells with an azide and the surface of tumor cells with a strained alkyne. The selective reactivity of these two groups provided the covalent binding of the two cell types in vivo, resulting in an enhanced tumor-specific immune response [61]. An analogous strategy was employed to promote the nanoparticle uptake by cancer tissues. Cai and coworkers functionalized—through metabolic incorporation with an azido-modified sugar—the plasma membrane of T-cells. This functionalization is achieved by incubating the cells with *N*-tetraacylated azido acetyl-galactosamine (Ac$_4$GalNAz) and harnessing the native glycometabolism (Figure 6) [62]. The azido-decor membrane is then extracted and used to wrap poly(lactic-*co*-glycolic)acid (PLGA) polymeric nanoparticles containing indocyanine green, generating the azido-labeled T-cell membrane-coated ICG-PLGA (N$_3$-TINP) biomimetic nanoparticles. In parallel, tumor-bearing mice are injected with acetylated *N*-bicyclo[6.1.0]non-4-yne (BCN)-acetyl-D-mannosamine (Ac$_4$ManN-BCN) to allow the tumor cell surface to be decorated with the BCN groups. After administration of the N$_3$-TINP nanoparticles, the in vivo SPAAC reaction with the BCN tumor cells increased the nanoparticle uptake and, consequently, the antitumor effect. As a result, the mice treated with N$_3$-TINP-treated mice showed more effective photothermal therapy with higher local temperature and tumor eradication. Importantly, no side effects were detected.
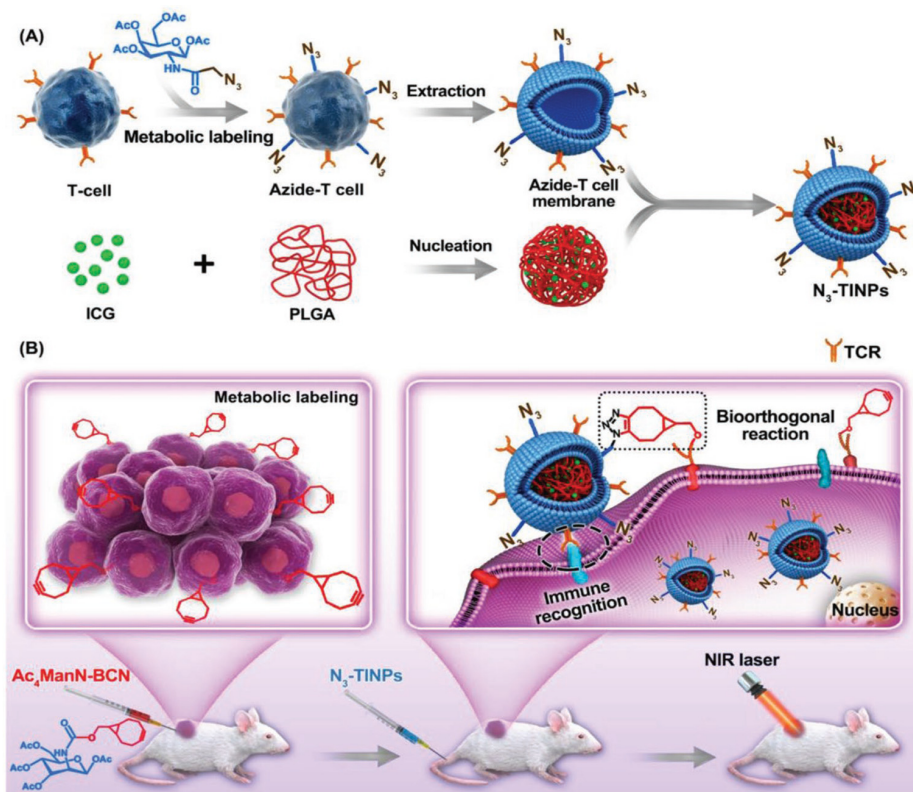

Figure 6. Schematic representation of the approach used by Cai and coworkers. (**A**) Generation of N$_3$-TINPs. The T cell surface is prior functionalized with azido-groups through metabolic incorporation

of Ac$_4$GalNAz. Subsequently, T cell membranes are extracted and used to coat pre-assembled ICG-PLGA cores. (**B**) Intratumor injection of Ac$_4$ManN-BCN led to tumor cell surface decoration with BCN via metabolic labeling. The following injection of N$_3$-TINPs particles resulted in the interaction with the tumor tissues both through immune recognition T cell membrane-tumor cells and BCN-N$_3$ SPAAC reaction. After laser irradiation, the tumor burden is reduced thanks to ICG-mediated photothermal therapy. Reprinted with permission from ref. [62]. Copyright 2019 The Authors. Published by WILEY-VCH.

The work from Qin and coworkers represents an elegant approach of in vivo SPAAC harnessed to enhance the immune response of an anticancer vaccine [63]. The research focused on developing an anticancer vaccine capable of targeting the lymph nodes-resident immune cells, to trigger a more robust and durable immune response against a specific antigen. First, the azido group was installed in the lymph nodes using (1,2-distearoyl-snglycero-3-phosphoethanolamine–poly(ethylene glycol)–azide) (DSPE-PEG-N$_3$). Such a polymer is capable, after intracutaneous injection, of binding the circulating albumin and, through an albumin hitchhiking mechanism, being transported to lymph nodes. Here, the polymer translocates from albumin to lymphatic endothelial cells' plasma membrane. As a result, multiple azido groups will be installed on the lymph node's internal surface (Figure 7). The full vaccination system, which includes the antigen peptide OVA257–264 from ovalbumin and the Toll-like receptor TLR agonist poly(I:C) adjuvant, was loaded into DBCO-modified liposomes. The injection of the vaccine-loaded DBCO-liposomes leads to the accumulation at the azide-functionalized lymph nodes endothelium thanks to the in situ SPAAC reaction. The strategy resulted in being particularly effective in (i) promoting high and specific localization of liposomes in the lymph nodes, (ii) activating strong immune signaling and T cell response, and (iii) leading to tumor regression in a syngeneic metastatic melanoma cancer model.
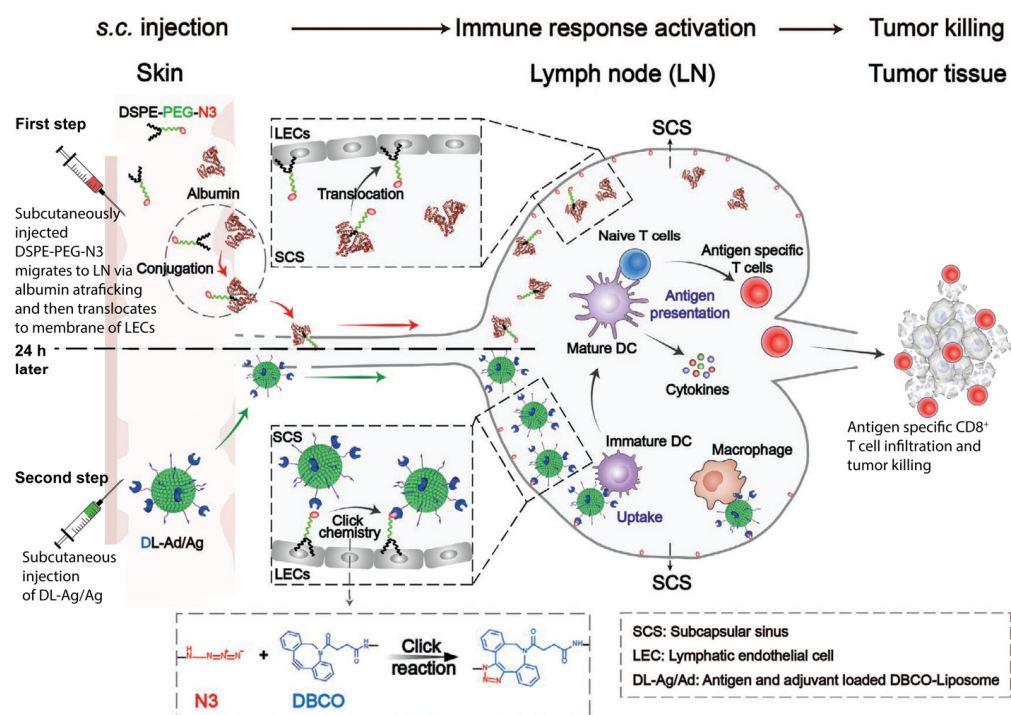

Figure 7. Schematic representation of the approach developed by Qin and coworkers. The first step is the administration of DSPE–PEG–N$_3$ through a subcutaneous injection. The DSPE group forms a

complex with interstitial albumin able to reach the lymph nodes. Once in the lymphatic system, DSPE–PEG–N_3 is largely distributed in the subcapsular sinus (SCS). Here, DSPE–PEG–N_3 translocates from albumin to lymphatic endothelial cells (LECs), generating a surface covered by azide groups available for subsequent SPAAC reaction. In a second administration step, antigen peptide/adjuvant-loaded liposomes, modified with a DBCO group on their surface, are subcutaneously administered to allow vaccine accumulation at lymph nodes at the endothelial level after the SPAAC reaction. The system provides highly efficient vaccine uptake by lymph nodes' immune cells, such as macrophages, generating a robust antigen-specific immune response against the tumor. Adapted with permission from ref. [63]. Copyright 2021 by WILEY-VCH.

In summary, these studies highlight the broad potential of SPAAC to perform coupling on reactions biomolecules, polymers, and nanostructures directly within living systems. The approaches also present the efficacy of the bioorthogonal mechanisms in biological interaction-mimicking strategies for in situ therapeutic applications.

4. Tetrazine Ligation (Inverse Electron-Demand Diels–Alder)

The tetrazine ligation is based on an Inverse Electron-Demand Diels–Alder (IEDDA) cycloaddition that occurs between a 1,2,4,5-tetrazine and a strained alkene, or alkyne, dienophile. The bioorthogonal nature of this coupling was presented in the initial study, together with its applicability in living systems [64]. This fast kinetic and the essential absence of byproducts of this mechanism are two key qualities for in vivo applications [53,65]. A frequently used tetrazine is the 6-phenyl-1,2,4,5-tetrazine having the molecule of interest at position 3. This group shows a good balance between reactivity and limited steric hindrance, also offering compatibility with biological systems [66]. As a dienophile, the *trans*-cyclooctene (TCO) is one of the typical strained alkenes employed. An added possibility with respect to other "click" cycloadditions is to use this reactivity for the "click-to-release" mechanism, with the possibility to "uncage" drug and dye molecules at the therapeutic site [67].

Hou and coworkers developed an efficient antibacterial strategy through IEDDA reaction between a tetrazine-modified Janus nanoparticle and TCO-labeled bacteria [68]. Janus nanoparticles can have two or more components and offer different surface properties for biomedical applications. In the study, the nanoparticles were composed of Au and $MnFe_2O_4$ (Au/MFO), resulting in magnetic properties with antibacterial and self-tracking properties (Figure 8).

In this work, the Au portion of the nanoparticles is functionalized with tetrazine via Au-S bonding. The nanoparticles were first treated with a mixture of mercapto polyethylene glycol-monomethyl ether (HS-PEG-OMe) and -amine (HS-PEG-NH_2) to generate an amino functionality that reacted with tetrazine-NHS to yield tetrazine-decorated nanoparticles. On the other side, the MFO portion exerts three different actions: First, a peroxidase activity, catalyzing the oxidation of the chromogenic substrate 3,3′,5,5′-tetramethylbenzidine by H_2O_2 and providing the nanoparticle self-tracking activity for quantifying bacteria. Furthermore, the magnetic property of the MFO is exploited for nanoparticle separation and to directly damage the bacterial membrane by magnetic heating with a high-frequency magnetic field. To promote the nanoparticle activity, a panel of Gram-positive bacteria (*Staphylococcus aureus*, *Bacillus subtilis*, *Enterococcus faecalis*, and *Streptococcus pyogenes*) was equipped with TCO groups on their surface, providing the chemical handle for grafting tetrazine-decorated therapeutic nanoparticles. To achieve the TCO decoration, bacteria were fed with D-lysine-PEG4-TCO, which metabolically incorporates the TCO in the terminal peptide of the peptidoglycan on the bacterial surface [69]. After one hour of incubation of TCO-tagged bacteria with tetrazine-modified nanoparticles to enable the "click" reaction, bacterial viability revealed a dose-dependent therapeutic result, showing the occurred coupling reaction. The observed effect is also significantly higher compared to the control bacteria treated with the nanoparticles lacking the tetrazine group. Overall, the quick reactivity of the tetrazine results in efficient bacterial killing while the peroxidase activity

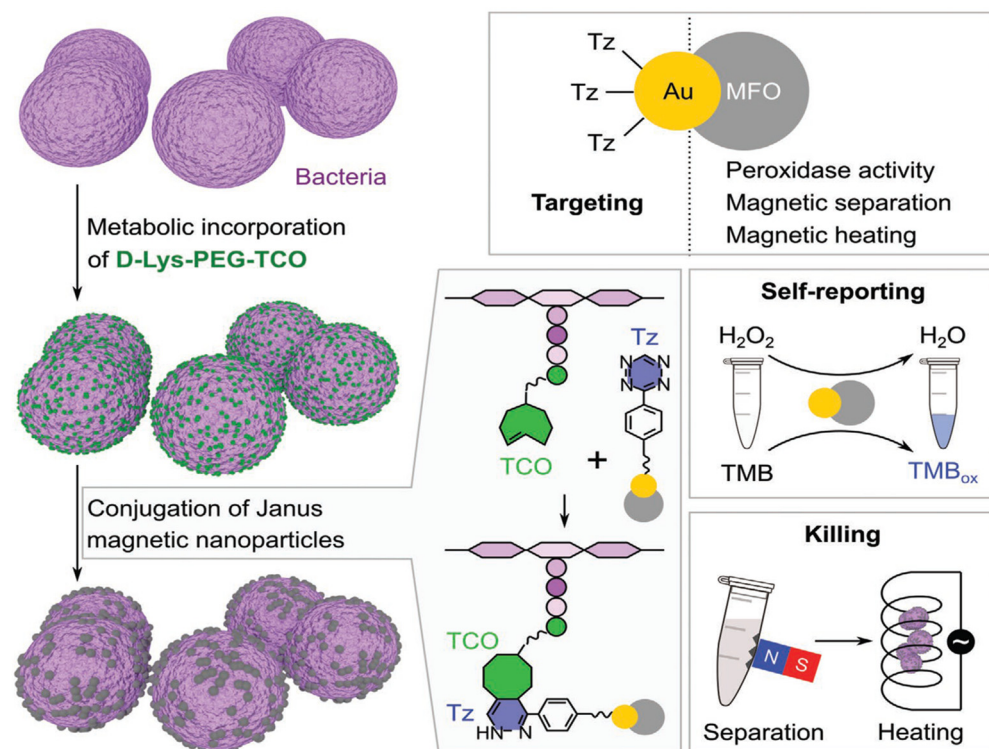of the MFO offers traceability for diagnostic applications, such as skin and urinary tract infections.

Figure 8. Antibacterial strategy developed by Hou and coworkers. Schematic representation of bacterial surface functionalization with TCO and in vivo conjugation with tetrazine-Janus magnetic nanoparticle through tetrazine ligation. The Au portion of the $Au/MnFe_2O_4$ Janus nanoparticles (Au/MFO) provides the backbone for tetrazine(Tz)-functionalization, while the MFO portion provides peroxidase activity (TMB = 3,3′,5,5′-tetramethylbenzidine), and its magnetic property allows for the magnetic separation, heating, and subsequent killing of the bacteria. Reprinted with permission from ref. [68]. Copyright 2020 by WILEY-VCH.

The application of the "click-to-release" mechanisms for the tetrazine ligation on nanomaterials was shown by Li and coworkers. The authors performed the decoration of carbon nanotubes to increase the specificity of tumor imaging and targeting. The approach consists of a two-step pre-targeting strategy: (i) Carbon nanotubes decorated with tetrazine groups were first injected, accumulating at the tumor site due to the enhanced permeability and retention effect and providing localized tetrazine groups. (ii) Subsequently, the TCO drug or TCO dye is administered to let the two counterparts meet and perform the IEDDA coupling in situ (Figure 9) [70]. The drug (doxorubicin) or dye (hemicyanine) molecules are bonded to the TCO group via a carbamate linker, enabling a spontaneous and responsive detachment after the IEDDA reaction in the biological environment. This particular design of the TCO–molecule conjugates allows them to shift from inactive to active form only after the in situ IEDDA reaction has occurred. In particular, the TCO–doxorubicin conjugate shows minimal toxicity levels compared to free doxorubicin. The TCO conjugation also masked the fluorescence of hemicyanine. The experiments were performed in vitro and in vivo on breast cancer models. The toxicity against the MCF-7 cell line was 25 times higher for cells pre-treated with tetrazine-SWCNT compared to the not pre-treated ones. The efficacy of the imaging approach was shown in vivo on CT26 xenografts mouse model where only the group pre-treated with tetrazine-nanotubes and administered with TCO-hemicyanine showed time-dependent tumor accumulation. In comparison, control groups showed a negligible signal as confirmed by ex vivo experiments. This tumor pre-targeting strategy employing carbon nanotubes as a delivery vehicle provided spatiotemporal control

for tumor sites over normal tissues. Taken together, the results highlight the potential of tetrazine-TCO "click" reaction for in vivo theragnostic applications.
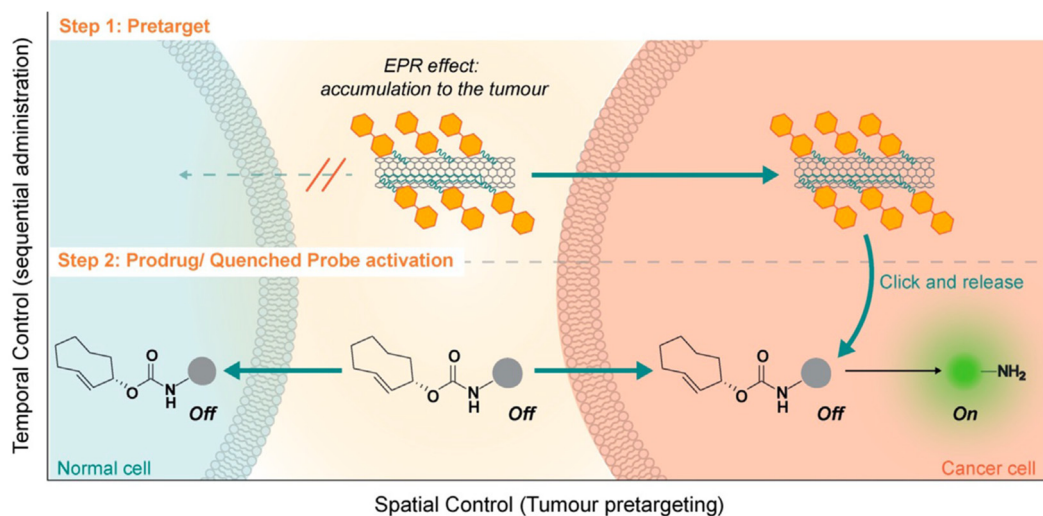

Figure 9. Schematic representation of the in situ "click-to-release" strategy for drug release in cancer cells. Tumor-bearing mice are pretreated with tetrazine-functionalized carbon nanotubes that accumulate selectively within tumor cells. The second injection of TCO-caged drug or fluorogenic dye allows the in situ release only after the IEDDA reaction in the so-called "click-to-release" approach. Reprinted with permission from ref. [70]. Copyright 2020 The Authors. Published by Wiley-VCH.

The tetrazine ligation was applied by Goos and coworkers for cancer imaging through the in situ decoration of star-shaped polymeric nanoparticles (nanostars) with a radiotracer [71]. Nanostars present a high functionalization potential, low viscosity, and small size. These nanoparticles also accumulate in cancer tissues through enhanced permeability and the retention effect, resulting in ideal vectors for theragnostic purposes. The nanostars were functionalized with TCO through PEG linkers and then coupled with two radiofluorinated tetrazines ([18F] F-Tz-PEG11-NODA and [18F] F-Tz-NODA), allowing for the in vivo biorthogonal IEDDA "click" reaction at the tumor site (Figure 10). Significantly, it was found that the reactivities of TCO- functionalized nanostars decreased with the increase in the PEG-linker length, as shown by PET imaging. This pre-targeting strategy enables separating the nanostar administration from the radioligand injection, improving tumor-to-background ratios and minimizing radiation exposure to healthy organs.
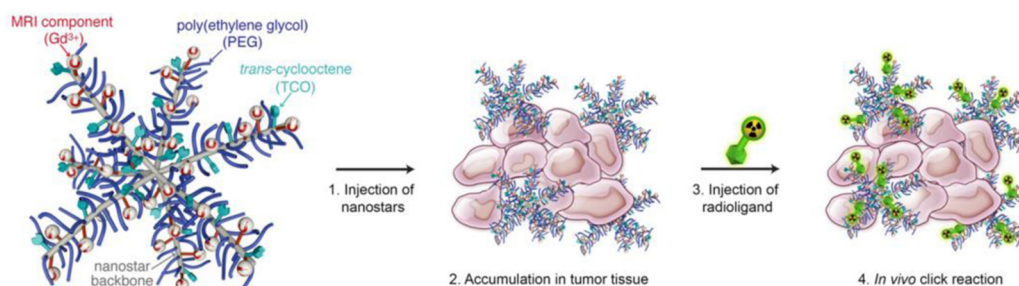

Figure 10. Graphical representation of the passive pre-targeting approach proposed by Goos and coworkers. The nanostars are composed of a polymeric backbone functionalized with a TCO group through a PEG linker of various sizes. The presence of gadolinium(III) (Gd^{3+}) is for the concomitant tracing detection by magnetic resonance imaging. After injection, TCO-functionalized nanostars passively accumulate at the tumor site. Subsequently, a tetrazine-functionalized radioligand is injected to obtain the selective binding to the TCO-functionalized nanostars and the PET imaging. Reprinted with permission from ref. [71]. Copyright 2020 Elsevier.

In traditional targeting methods based on biological ligands, tumor heterogeneity and limited expression of receptors challenge the theragnostic strategies. Guihong and coworkers developed a two-step tumor targeting using the IEDDA reaction aimed at overcoming these limitations. The approach relies on a modified peptide capable of cell membrane accumulation at low pH through C-terminus insertion (tetrazine-pHLIP, Figure 11) [72].
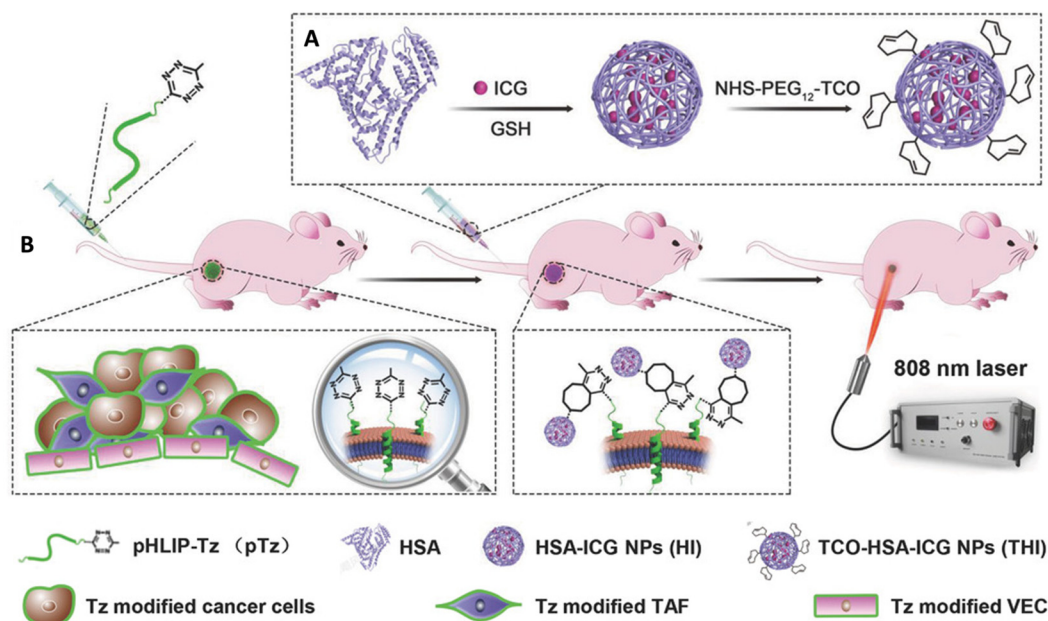

Figure 11. Schematic representation of the IEDDA-based two-step tumor-targeting strategy employed by Guihong and coworkers. (**A**) Preparation of indocyanine green-loaded serum albumin nanoparticles functionalized with TCO group (THI); Glutathione (GSH) protects cells from phototherapy-induced reactive oxygen species (ROS). (**B**) Tetrazine-modified pH (low) insertion peptides (pHLIP-Tz) (pTz) accumulate at the tumor site by incorporation into the cell membrane in a pH-dependent manner. These insertions provide chemical handles on the cell surface of cancer cells, vascular endothelial cells (VEC), and tumor-associated fibroblasts (TAF). The tetrazine groups are used as baits for THI through the IEDDA reaction with TCO. Then, THI mediates photothermal therapy after NIR laser irradiation. Reprinted with permission from ref. [72]. Copyright 2018 WILEY-VCH.

The coupling of the *N*-terminus tetrazine-derivative of the peptide with the tetrazine chemical handle occurred selectively in tumor tissues, as demonstrated by the IEDDA reaction in the in vivo xenograft mouse model. The efficacy of the pH dependance and in situ reactivity were performed on different cancer cell lines (HeLa, HUVEC, and NIH 3T3) pretreated with tetrazine-pHLIP at pH 6.2 and 7.4. Only the cells incubated at pH 6.2 showed fluorescence after treatment with a TCO-fluorophore (TCO-Cy5). The tumor accumulation of tetrazine-pHLIP was observed in vivo by histological TCO-Cy5 staining of various organs on a tumor xenograft mouse model. As an effector for the theragnostic approach, indocyanine green-loaded serum albumin nanoparticles functionalized with the TCO group (denoted as THI) were prepared. The in vivo photothermal efficiency from the indocyanine green-loaded nanoparticles was explored after NIR laser irradiation on a tumor xenograft mouse model. Notably, the complete tumor ablation was achieved after a single application of the proposed treatment, with minimal tumor regrowth. This two-step approach enhanced tumor-selective accumulation, improving photothermal therapy efficiency without significant toxicity for healthy tissues.

A further type of "click" cycloaddition that is worth to be mentioned is the nitrone-alkyne one. The explored applications of this reaction on nanostructures involve the coupling step before the effective administration to the living environment. However,

several studies offer a high potential for conducting the decoration of the nanostructures and polymers directly inside cells and biosystems [73–75].

5. Summary and Outlook

The recent development of bioorthogonal reactions opened a plethora of new opportunities for enhancing the outcome and specificity of nanomedicine-based treatments. "Click" cycloadditions demonstrated the ability to operate inside bioenvironments for increasing the targeting of desired tissues, the tissue-specific drug release, and the specificity of imaging agents. Bioorthogonal "click" cycloadditions offer selectivity, fast kinetics, and biocompatibility, making them ideal tools for chemistry in living systems. In this minireview, we presented the three fundamental types of bioorthogonal "click" cycloadditions to operate transformations on nanostructures and polymers, directly in biosystems: SPSAC, SPAAC, and tetrazine-TCO ligation. The presented research frames a reactivity also aimed at overcoming the limitations of various classical chemotherapies, including off-target toxicity and lack of spatiotemporal control. The use of these cycloadditions in biological studies has rapidly increased in recent decades and is expected to expand further. We envision that their use will offer a growing number of examples in living organisms, further expanding the foundation for improved therapeutic approaches.

Author Contributions: Conceptualization, guiding of the activity, writing, and coordination of the authors, S.F.; writing, review, and editing, I.L.; writing Y.O., J.I., N.G., M.P. and U.S.S. All authors have read and agreed to the published version of the manuscript.

Conflicts of Interest: The authors declare no conflicts of interest.

References

1. Sandreschi, S.; Piras, A.M.; Batoni, G.; Chiellini, F. Perspectives on Polymeric Nanostructures for the Therapeutic Application of Antimicrobial Peptides. *Nanomedicine* **2016**, *11*, 1729–1744. [CrossRef] [PubMed]
2. Bauri, S.; Tripathi, S.; Choudhury, A.M.; Mandal, S.S.; Raj, H.; Maiti, P. Nanomaterials as Theranostic Agents for Cancer Therapy. *ACS Appl. Nano Mater.* **2023**, *6*, 21462–21495. [CrossRef]
3. Ashkarran, A.A.; Lin, Z.; Rana, J.; Bumpers, H.; Sempere, L.; Mahmoudi, M. Impact of Nanomedicine in Women's Metastatic Breast Cancer. *Small* **2023**, 2301385. [CrossRef] [PubMed]
4. Krukiewicz, K.; Zak, J.K. Biomaterial-Based Regional Chemotherapy: Local Anticancer Drug Delivery to Enhance Chemotherapy and Minimize Its Side-Effects. *Mater. Sci. Eng. C* **2016**, *62*, 927–942. [CrossRef] [PubMed]
5. Negwer, I.; Best, A.; Schinnerer, M.; Schäfer, O.; Capeloa, L.; Wagner, M.; Schmidt, M.; Mailänder, V.; Helm, M.; Barz, M.; et al. Monitoring Drug Nanocarriers in Human Blood by Near-Infrared Fluorescence Correlation Spectroscopy. *Nat. Commun.* **2018**, *9*, 5306. [CrossRef] [PubMed]
6. Verde-Sesto, E.; Arbe, A.; Moreno, A.J.; Cangialosi, D.; Alegría, A.; Colmenero, J.; Pomposo, J.A. Single-Chain Nanoparticles: Opportunities Provided by Internal and External Confinement. *Mater. Horiz.* **2020**, *7*, 2292–2313. [CrossRef]
7. Wang, Z.; Niu, G.; Chen, X. Polymeric Materials for Theranostic Applications. *Pharm. Res.* **2014**, *31*, 1358–1376. [CrossRef]
8. Khan, M.I.; Hossain, M.I.; Hossain, M.K.; Rubel, M.H.K.; Hossain, K.M.; Mahfuz, A.M.U.B.; Anik, M.I. Recent Progress in Nanostructured Smart Drug Delivery Systems for Cancer Therapy: A Review. *ACS Appl. Bio Mater.* **2022**, *5*, 971–1012. [CrossRef]
9. Piotrowski-Daspit, A.S.; Kauffman, A.C.; Bracaglia, L.G.; Saltzman, W.M. Polymeric Vehicles for Nucleic Acid Delivery. *Adv. Drug Deliv. Rev.* **2020**, *156*, 119–132. [CrossRef]
10. Kang, X.; Wei, X.; Xiang, P.; Tian, X.; Zuo, Z.; Song, F.; Wang, S.; Zhu, M. Rendering Hydrophobic Nanoclusters Water-Soluble and Biocompatible. *Chem. Sci.* **2020**, *11*, 4808–4816. [CrossRef]
11. Majeed, M.I.; Lu, Q.; Yan, W.; Li, Z.; Hussain, I.; Tahir, M.N.; Tremel, W.; Tan, B. Highly Water-Soluble Magnetic Iron Oxide (Fe_3O_4) Nanoparticles for Drug Delivery: Enhanced in Vitro Therapeutic Efficacy of Doxorubicin and MION Conjugates. *J. Mater. Chem. B* **2013**, *1*, 2874. [CrossRef]
12. Amoozgar, Z.; Yeo, Y. Recent Advances in Stealth Coating of Nanoparticle Drug Delivery Systems. *WIREs Nanomed. Nanobiotechnology* **2012**, *4*, 219–233. [CrossRef]
13. Xu, Z.; Zhu, S.; Wang, M.; Li, Y.; Shi, P.; Huang, X. Delivery of Paclitaxel Using PEGylated Graphene Oxide as a Nanocarrier. *ACS Appl. Mater. Interfaces* **2015**, *7*, 1355–1363. [CrossRef] [PubMed]
14. Eslami, P.; Rossi, F.; Fedeli, S. Hybrid Nanogels: Stealth and Biocompatible Structures for Drug Delivery Applications. *Pharmaceutics* **2019**, *11*, 71. [CrossRef] [PubMed]

15. Wolfbeis, O.S. An Overview of Nanoparticles Commonly Used in Fluorescent Bioimaging. *Chem. Soc. Rev.* **2015**, *44*, 4743–4768. [CrossRef]

16. Fedeli, S.; Paoli, P.; Brandi, A.; Venturini, L.; Giambastiani, G.; Tuci, G.; Cicchi, S. Azido-Substituted BODIPY Dyes for the Production of Fluorescent Carbon Nanotubes. *Chem. A Eur. J.* **2015**, *21*, 15349–15353. [CrossRef] [PubMed]

17. Liu, L.; Wang, X.; Zhu, S.; Li, L. Different Surface Interactions between Fluorescent Conjugated Polymers and Biological Targets. *ACS Appl. Bio Mater.* **2021**, *4*, 1211–1220. [CrossRef]

18. Kaplun, V.; Stepensky, D. Efficient Decoration of Nanoparticles Intended for Intracellular Drug Targeting with Targeting Residues, as Revealed by a New Indirect Analytical Approach. *Mol. Pharm.* **2014**, *11*, 2906–2914. [CrossRef]

19. Barui, A.K.; Oh, J.Y.; Jana, B.; Kim, C.; Ryu, J. Cancer-Targeted Nanomedicine: Overcoming the Barrier of the Protein Corona. *Adv. Ther.* **2020**, *3*, 1900124. [CrossRef]

20. Taghavi, S.; Ramezani, M.; Alibolandi, M.; Abnous, K.; Taghdisi, S.M. Chitosan-Modified PLGA Nanoparticles Tagged with 5TR1 Aptamer for in Vivo Tumor-Targeted Drug Delivery. *Cancer Lett.* **2017**, *400*, 1–8. [CrossRef]

21. Hsu, P.-H.; Almutairi, A. Recent Progress of Redox-Responsive Polymeric Nanomaterials for Controlled Release. *J. Mater. Chem. B* **2021**, *9*, 2179–2188. [CrossRef] [PubMed]

22. Seidi, F.; Jenjob, R.; Crespy, D. Designing Smart Polymer Conjugates for Controlled Release of Payloads. *Chem. Rev.* **2018**, *118*, 3965–4036. [CrossRef] [PubMed]

23. Kamaly, N.; Yameen, B.; Wu, J.; Farokhzad, O.C. Degradable Controlled-Release Polymers and Polymeric Nanoparticles: Mechanisms of Controlling Drug Release. *Chem. Rev.* **2016**, *116*, 2602–2663. [CrossRef] [PubMed]

24. Indoria, S.; Singh, V.; Hsieh, M.-F. Recent Advances in Theranostic Polymeric Nanoparticles for Cancer Treatment: A Review. *Int. J. Pharm.* **2020**, *582*, 119314. [CrossRef] [PubMed]

25. Jaymand, M. Chemically Modified Natural Polymer-Based Theranostic Nanomedicines: Are They the Golden Gate toward a de Novo Clinical Approach against Cancer? *ACS Biomater. Sci. Eng.* **2020**, *6*, 134–166. [CrossRef]

26. Paramasivam, G.; Sanmugam, A.; Palem, V.V.; Sevanan, M.; Sairam, A.B.; Nachiappan, N.; Youn, B.; Lee, J.S.; Nallal, M.; Park, K.H. Nanomaterials for Detection of Biomolecules and Delivering Therapeutic Agents in Theragnosis: A Review. *Int. J. Biol. Macromol.* **2024**, *254*, 127904. [CrossRef] [PubMed]

27. Kang, R.H.; Kim, Y.; Kim, J.H.; Kim, N.H.; Ko, H.M.; Lee, S.-H.; Shim, I.; Kim, J.S.; Jang, H.-J.; Kim, D. Self-Activating Therapeutic Nanoparticle: A Targeted Tumor Therapy Using Reactive Oxygen Species Self-Generation and Switch-on Drug Release. *ACS Appl. Mater. Interfaces* **2021**, *13*, 30359–30372. [CrossRef]

28. Pan, Q.; Peng, X.; Cun, J.-E.; Li, J.; Pu, Y.; He, B. In-Situ Drug Generation and Controllable Loading: Rational Design of Copper-Based Nanosystems for Chemo-Photothermal Cancer Therapy. *Chem. Eng. J.* **2021**, *409*, 128222. [CrossRef]

29. Fedeli, S.; Im, J.; Gopalakrishnan, S.; Elia, J.L.; Gupta, A.; Kim, D.; Rotello, V.M. Nanomaterial-Based Bioorthogonal Nanozymes for Biological Applications. *Chem. Soc. Rev.* **2021**, *50*, 13467–13480. [CrossRef]

30. Hirschbiegel, C.-M.; Zhang, X.; Huang, R.; Cicek, Y.A.; Fedeli, S.; Rotello, V.M. Inorganic Nanoparticles as Scaffolds for Bioorthogonal Catalysts. *Adv. Drug Deliv. Rev.* **2023**, *195*, 114730. [CrossRef]

31. Biju, V. Chemical Modifications and Bioconjugate Reactions of Nanomaterials for Sensing, Imaging, Drug Delivery and Therapy. *Chem. Soc. Rev.* **2014**, *43*, 744–764. [CrossRef]

32. Tuci, G.; Luconi, L.; Rossin, A.; Baldini, F.; Cicchi, S.; Tombelli, S.; Trono, C.; Giannetti, A.; Manet, I.; Fedeli, S.; et al. A Hetero-Bifunctional Spacer for the Smart Engineering of Carbon-Based Nanostructures. *Chempluschem* **2015**, *80*, 704–714. [CrossRef] [PubMed]

33. Heinz, H.; Pramanik, C.; Heinz, O.; Ding, Y.; Mishra, R.K.; Marchon, D.; Flatt, R.J.; Estrela-Lopis, I.; Llop, J.; Moya, S.; et al. Nanoparticle Decoration with Surfactants: Molecular Interactions, Assembly, and Applications. *Surf. Sci. Rep.* **2017**, *72*, 1–58. [CrossRef]

34. Chatterjee, M.; Chanda, N. Formulation of PLGA Nano-Carriers: Specialized Modification for Cancer Therapeutic Applications. *Mater. Adv.* **2022**, *3*, 837–858. [CrossRef]

35. Sletten, E.M.; Bertozzi, C.R. Bioorthogonal Chemistry: Fishing for Selectivity in a Sea of Functionality. *Angew. Chem. Int. Ed.* **2009**, *48*, 6974–6998. [CrossRef] [PubMed]

36. Nguyen, S.S.; Prescher, J.A. Developing Bioorthogonal Probes to Span a Spectrum of Reactivities. *Nat. Rev. Chem.* **2020**, *4*, 476–489. [CrossRef] [PubMed]

37. Taiariol, L.; Chaix, C.; Farre, C.; Moreau, E. Click and Bioorthogonal Chemistry: The Future of Active Targeting of Nanoparticles for Nanomedicines? *Chem. Rev.* **2022**, *122*, 340–384. [CrossRef] [PubMed]

38. Yi, W.; Xiao, P.; Liu, X.; Zhao, Z.; Sun, X.; Wang, J.; Zhou, L.; Wang, G.; Cao, H.; Wang, D.; et al. Recent Advances in Developing Active Targeting and Multi-Functional Drug Delivery Systems via Bioorthogonal Chemistry. *Signal Transduct. Target. Ther.* **2022**, *7*, 386. [CrossRef] [PubMed]

39. Deb, T.; Tu, J.; Franzini, R.M. Mechanisms and Substituent Effects of Metal-Free Bioorthogonal Reactions. *Chem. Rev.* **2021**, *121*, 6850–6914. [CrossRef]

40. Wu, D.; Yang, K.; Zhang, Z.; Feng, Y.; Rao, L.; Chen, X.; Yu, G. Metal-Free Bioorthogonal Click Chemistry in Cancer Theranostics. *Chem. Soc. Rev.* **2022**, *51*, 1336–1376. [CrossRef]

41. Franc, G.; Kakkar, A.K. "Click" Methodologies: Efficient, Simple and Greener Routes to Design Dendrimers. *Chem. Soc. Rev.* **2010**, *39*, 1536. [CrossRef]

42.   Fedeli, S.; Brandi, A.; Venturini, L.; Chiarugi, P.; Giannoni, E.; Paoli, P.; Corti, D.; Giambastiani, G.; Tuci, G.; Cicchi, S. The "Click-on-Tube" Approach for the Production of Efficient Drug Carriers Based on Oxidized Multi-Walled Carbon Nanotubes. *J. Mater. Chem. B* **2016**, *4*, 3823–3831. [CrossRef]

43.   Liu, Y.; Hou, W.; Sun, H.; Cui, C.; Zhang, L.; Jiang, Y.; Wu, Y.; Wang, Y.; Li, J.; Sumerlin, B.S.; et al. Thiol–Ene Click Chemistry: A Biocompatible Way for Orthogonal Bioconjugation of Colloidal Nanoparticles. *Chem. Sci.* **2017**, *8*, 6182–6187. [CrossRef]

44.   Jewett, J.C.; Bertozzi, C.R. Cu-Free Click Cycloaddition Reactions in Chemical Biology. *Chem. Soc. Rev.* **2010**, *39*, 1272. [CrossRef]

45.   Wallace, S.; Chin, J.W. Strain-Promoted Sydnone Bicyclo-[6.1.0]-Nonyne Cycloaddition. *Chem. Sci.* **2014**, *5*, 1742–1744. [CrossRef]

46.   Dommerholt, J.; van Rooijen, O.; Borrmann, A.; Guerra, C.F.; Bickelhaupt, F.M.; van Delft, F.L. Highly Accelerated Inverse Electron-Demand Cycloaddition of Electron-Deficient Azides with Aliphatic Cyclooctynes. *Nat. Commun.* **2014**, *5*, 5378. [CrossRef] [PubMed]

47.   Plougastel, L.; Koniev, O.; Specklin, S.; Decuypere, E.; Créminon, C.; Buisson, D.-A.; Wagner, A.; Kolodych, S.; Taran, F. 4-Halogeno-Sydnones for Fast Strain Promoted Cycloaddition with Bicyclo-[6.1.0]-Nonyne. *Chem. Commun.* **2014**, *50*, 9376–9378. [CrossRef] [PubMed]

48.   Richard, M.; Truillet, C.; Tran, V.L.; Liu, H.; Porte, K.; Audisio, D.; Roche, M.; Jego, B.; Cholet, S.; Fenaille, F.; et al. New Fluorine-18 Pretargeting PET Imaging by Bioorthogonal Chlorosydnone–Cycloalkyne Click Reaction. *Chem. Commun.* **2019**, *55*, 10400–10403. [CrossRef] [PubMed]

49.   Gerke, C.; Zabala Gutierrez, I.; Méndez-González, D.; la Cruz, M.C.I.; Mulero, F.; Jaque, D.; Rubio-Retama, J. Clickable Albumin Nanoparticles for Pretargeted Drug Delivery toward PD-L1 Overexpressing Tumors in Combination Immunotherapy. *Bioconjug. Chem.* **2022**, *33*, 821–828. [CrossRef] [PubMed]

50.   Chinoy, Z.S.; Bodineau, C.; Favre, C.; Moremen, K.W.; Durán, R.V.; Friscourt, F. Selective Engineering of Linkage-Specific A2,6- N-Linked Sialoproteins Using Sydnone-Modified Sialic Acid Bioorthogonal Reporters. *Angew. Chem. Int. Ed.* **2019**, *58*, 4281–4285. [CrossRef]

51.   Krell, K.; Pfeuffer, B.; Rönicke, F.; Chinoy, Z.S.; Favre, C.; Friscourt, F.; Wagenknecht, H. Fast and Efficient Postsynthetic DNA Labeling in Cells by Means of Strain-Promoted Sydnone-Alkyne Cycloadditions. *Chem. A Eur. J.* **2021**, *27*, 16093–16097. [CrossRef]

52.   Agard, N.J.; Prescher, J.A.; Bertozzi, C.R. A Strain-Promoted [3 + 2] Azide−Alkyne Cycloaddition for Covalent Modification of Biomolecules in Living Systems. *J. Am. Chem. Soc.* **2004**, *126*, 15046–15047. [CrossRef]

53.   Bird, R.E.; Lemmel, S.A.; Yu, X.; Zhou, Q.A. Bioorthogonal Chemistry and Its Applications. *Bioconjug Chem.* **2021**, *32*, 2457–2479. [CrossRef]

54.   Wu, F.; Liu, J. Decorated Bacteria and the Application in Drug Delivery. *Adv. Drug. Deliv. Rev.* **2022**, *188*, 114443. [CrossRef] [PubMed]

55.   Debets, M.F.; van der Doelen, C.W.; Rutjes, F.P.; van Delft, F.L. Azide: A Unique Dipole for Metal-Free Bioorthogonal Ligations. *Chembiochem* **2010**, *11*, 1168–1184. [CrossRef]

56.   Wang, Y.; Huang, G.; Hou, Q.; Pan, H.; Cai, L. Cell Surface-nanoengineering for Cancer Targeting Immunoregulation and Precise Immunotherapy. *WIREs Nanomed. Nanobiotechnology* **2023**, *15*, e1875. [CrossRef] [PubMed]

57.   Zeng, X.; Li, P.; Yan, S.; Liu, B.-F. Reduction/pH-Responsive Disassemblable MOF-Microbial Nanohybrid for Targeted Tumor Penetration and Synergistic Therapy. *Chem. Eng. J.* **2023**, *452*, 139517. [CrossRef]

58.   Zhou, S.; Gravekamp, C.; Bermudes, D.; Liu, K. Tumour-Targeting Bacteria Engineered to Fight Cancer. *Nat. Rev. Cancer* **2018**, *18*, 727–743. [CrossRef]

59.   Siegrist, M.S.; Whiteside, S.; Jewett, J.C.; Aditham, A.; Cava, F.; Bertozzi, C.R. d-Amino Acid Chemical Reporters Reveal Peptidoglycan Dynamics of an Intracellular Pathogen. *ACS Chem. Biol.* **2013**, *8*, 500–505. [CrossRef]

60.   Wang, Y.; Li, Z.; Mo, F.; Chen-Mayfield, T.J.; Saini, A.; LaMere, A.M.; Hu, Q. Chemically Engineering Cells for Precision Medicine. *Chem. Soc. Rev.* **2023**, *52*, 1068–1102. [CrossRef] [PubMed]

61.   Pan, H.; Li, W.; Chen, Z.; Luo, Y.; He, W.; Wang, M.; Tang, X.; He, H.; Liu, L.; Zheng, M.; et al. Click CAR-T Cell Engineering for Robustly Boosting Cell Immunotherapy in Blood and Subcutaneous Xenograft Tumor. *Bioact. Mater.* **2021**, *6*, 951–962. [CrossRef]

62.   Han, Y.; Pan, H.; Li, W.; Chen, Z.; Ma, A.; Yin, T.; Liang, R.; Chen, F.; Ma, Y.; Jin, Y.; et al. T Cell Membrane Mimicking Nanoparticles with Bioorthogonal Targeting and Immune Recognition for Enhanced Photothermal Therapy. *Adv. Sci.* **2019**, *6*, 1900251. [CrossRef] [PubMed]

63.   Qin, H.; Zhao, R.; Qin, Y.; Zhu, J.; Chen, L.; Di, C.; Han, X.; Cheng, K.; Zhang, Y.; Zhao, Y.; et al. Development of a Cancer Vaccine Using In Vivo Click-Chemistry-Mediated Active Lymph Node Accumulation for Improved Immunotherapy. *Adv. Mater.* **2021**, *33*, e2006007. [CrossRef] [PubMed]

64.   Devaraj, N.K.; Weissleder, R.; Hilderbrand, S.A. Tetrazine-Based Cycloadditions: Application to Pretargeted Live Cell Imaging. *Bioconjug Chem.* **2008**, *19*, 2297–2299. [CrossRef] [PubMed]

65.   Scinto, S.L.; Bilodeau, D.A.; Hincapie, R.; Lee, W.; Nguyen, S.S.; Xu, M.; Am Ende, C.W.; Finn, M.G.; Lang, K.; Lin, Q.; et al. Bioorthogonal Chemistry. *Nat. Rev. Methods Prim.* **2021**, *1*, 30. [CrossRef] [PubMed]

66.   Oliveira, B.L.; Guo, Z.; Bernardes, G.J.L. Inverse Electron Demand Diels-Alder Reactions in Chemical Biology. *Chem. Soc. Rev.* **2017**, *46*, 4895–4950. [CrossRef] [PubMed]

67.   Porte, K.; Riberaud, M.; Châtre, R.; Audisio, D.; Papot, S.; Taran, F. Bioorthogonal Reactions in Animals. *ChemBioChem* **2021**, *22*, 100–113. [CrossRef] [PubMed]

68.   Hou, S.; Mahadevegowda, S.H.; Lu, D.; Zhang, K.; Chan-Park, M.B.; Duan, H. Metabolic Labeling Mediated Targeting and Thermal Killing of Gram-Positive Bacteria by Self-Reporting Janus Magnetic Nanoparticles. *Small* **2021**, *17*, e2006357. [CrossRef]

69.   Fura, J.M.; Kearns, D.; Pires, M.M. D-Amino Acid Probes for Penicillin Binding Protein-Based Bacterial Surface Labeling. *J. Biol. Chem.* **2015**, *290*, 30540–30550. [CrossRef]

70.   Li, H.; Conde, J.; Guerreiro, A.; Bernardes, G.J.L. Tetrazine Carbon Nanotubes for Pretargeted In Vivo "Click-to-Release" Bioorthogonal Tumour Imaging. *Angew. Chem. Int. Ed.* **2020**, *59*, 16023–16032. [CrossRef]

71.   Goos, J.; Davydova, M.; Dilling, T.R.; Cho, A.; Cornejo, M.A.; Gupta, A.; Price, W.S.; Puttick, S.; Whittaker, M.R.; Quinn, J.F.; et al. Design and Preclinical Evaluation of Nanostars for the Passive Pretargeting of Tumor Tissue. *Nucl. Med. Biol.* **2020**, *84–85*, 63–72. [CrossRef]

72.   Lu, G.; Li, F.; Zhang, F.; Huang, L.; Zhang, L.; Lv, Y.; Wei, W.; Xie, H. Amplifying Nanoparticle Targeting Performance to Tumor via Diels–Alder Cycloaddition. *Adv. Funct. Mater.* **2018**, *28*, 1707596. [CrossRef]

73.   MacKenzie, D.A.; Sherratt, A.R.; Chigrinova, M.; Kell, A.J.; Pezacki, J.P. Bioorthogonal Labelling of Living Bacteria Using Unnatural Amino Acids Containing Nitrones and a Nitrone Derivative of Vancomycin. *Chem. Commun.* **2015**, *51*, 12501–12504. [CrossRef] [PubMed]

74.   Colombo, M.; Sommaruga, S.; Mazzucchelli, S.; Polito, L.; Verderio, P.; Galeffi, P.; Corsi, F.; Tortora, P.; Prosperi, D. Site-Specific Conjugation of ScFvs Antibodies to Nanoparticles by Bioorthogonal Strain-Promoted Alkyne–Nitrone Cycloaddition. *Angew. Chem. Int. Ed.* **2012**, *51*, 496–499. [CrossRef] [PubMed]

75.   MacKenzie, D.A.; Sherratt, A.R.; Chigrinova, M.; Cheung, L.L.; Pezacki, J.P. Strain-Promoted Cycloadditions Involving Nitrones and Alkynes—Rapid Tunable Reactions for Bioorthogonal Labeling. *Curr. Opin. Chem. Biol.* **2014**, *21*, 81–88. [CrossRef]